

## Photoluminescence from Si nanocrystals induced by high-temperature implantation in SiO<sub>2</sub>

U. S. Sias, E. C. Moreira, E. Ribeiro, H. Boudinov, L. Amaral, and M. Behar

Citation: *Journal of Applied Physics* **95**, 5053 (2004); doi: 10.1063/1.1691182

View online: <http://dx.doi.org/10.1063/1.1691182>

View Table of Contents: <http://scitation.aip.org/content/aip/journal/jap/95/9?ver=pdfcov>

Published by the [AIP Publishing](#)

---



## Re-register for Table of Content Alerts

Create a profile.



Sign up today!



# Photoluminescence from Si nanocrystals induced by high-temperature implantation in SiO<sub>2</sub>

U. S. Sias

*Instituto de Física, Universidade Federal do Rio Grande do Sul, Caixa Postal, 91501-970 Porto Alegre, Brazil and Centro Federal de Educação Tecnológica, Pelotas-RS, Brazil*

E. C. Moreira

*Universidade Estadual do Rio Grande do Sul, Unidade de Guaíba, Guaíba-RS, Brazil*

E. Ribeiro

*Laboratório Nacional de Luz Síncrotron, CP-6192, 13084-971 Campinas-SP, Brazil*

H. Boudinov, L. Amaral, and M. Behar<sup>a)</sup>

*Instituto de Física, Universidade Federal do Rio Grande do Sul, Caixa Postal 15051, 91501-970 Porto Alegre-RS, Brazil*

(Received 6 October 2003; accepted 11 February 2004)

A systematic study of photoluminescence (PL) behavior of Si nanocrystals in SiO<sub>2</sub> obtained by ion implantation in a large range of temperatures (−200 up to 800 °C), and subsequent furnace annealing in N<sub>2</sub> ambient was performed. A PL signal in the wavelength range 650–1000 nm was observed. The PL peak wavelength and intensity are dependent on the fluence, implantation and annealing temperatures. It was found that after annealing at 1100 °C, both implantations of  $1.5 \times 10^{17}$  Si/cm<sup>2</sup> at room temperature or  $0.5 \times 10^{17}$  Si/cm<sup>2</sup> at 400 °C result in the same PL peak intensity. By varying the implantation temperature we can achieve the same PL efficiency with lower fluences showing that hot implantations play an important role for initial formation of the nanocrystals. The PL intensity evolution as a function of the annealing time was also studied. As the implantation temperature was increased, larger mean size Si nanocrystals were observed by means of dark-field transmission electron microscopy analysis. © 2004 American Institute of Physics. [DOI: 10.1063/1.1691182]

## I. INTRODUCTION

Silicon nanocrystals (NCs) have been extensively studied in recent years due their potential applications in optoelectronic and photonic devices. Most researchers have sought an understanding of the light-emission process, and the enhancement of the emission efficiency of these systems. In spite of a great amount of publications, there is still no consensus about the luminescence mechanism. The discussions are basically centered on whether light emission occurs via quantum confinement or via interface states localized in the NC surface. More recently, the so-called reactive model of nanoclusters has been proposed.<sup>1</sup> The authors have considered that the bandgap widening due to the quantum confinement effect plays a role in the photoabsorption process, and that the Si-NC/SiO<sub>2</sub> interface energy states plays an essential role in the luminescence process. The nonexistence of a well-accepted model to explain the luminescence from Si NC is strictly associated with the wide range of sometimes conflicting experimental results available in the literature. For instance, intense light emission from as-deposited SiO<sub>x</sub> films has been reported,<sup>2</sup> although the results of most of the experiments agree that high-temperature thermal treatment of the films ( $T > 1000$  °C) is necessary in order to observe

significant light emission.<sup>3,4</sup> Some authors report a dependence of the photoluminescence (PL) peak wavelength on the annealing temperature and/or the films composition, while others do not observe any dependence.<sup>1,2,5</sup> Some publications have shown that long annealing times (about hours) produce an increase in the PL intensity,<sup>6</sup> while others have reported a decrease in the PL intensity peak<sup>7</sup> and some authors have observed saturation in Si NC PL.<sup>8</sup> In most of the published papers, the emission spectra shape is not related to the wavelength excitation source.

A variety of techniques has been employed to produce nanometer-sized crystallites.<sup>9–20</sup> By modifying the way that the initial silicon excess is generated (usually) in a SiO<sub>2</sub> matrix by different annealing ambient conditions, one can obtain different structural and optical characteristics. Ion implantation can be considered one of the best ways to generate this silicon excess, due to the excellent repeatability and compatibility with conventional microelectronic technology. Ion implantation at keV energies is routine for microelectronic applications, and it has the advantage that a given concentration of ions can be placed in a controlled depth distribution by changing the ion fluence and the implantation energy.

Si NCs embedded in a SiO<sub>2</sub> matrix are usually studied as a function of the implantation fluence and the annealing parameters such as time and temperature.<sup>4,3,6,13</sup> In the present

<sup>a)</sup> Author to whom correspondence should be addressed; electronic mail: behar@if.ufrgs.br

work, we focus on the influence of the implantation temperature on the nanocrystal's structural and emission characteristics, an issue that has never been systematically studied.

## II. EXPERIMENTAL DETAILS

Silicon ions with energy of 170 keV were implanted in 480-nm-thick SiO<sub>2</sub> layers thermally grown on (100) Si wafers. These implantations were carried out in a range of target temperatures, between  $-200$  and  $800$  °C, in a vacuum better than  $1 \times 10^{-6}$  mbar. We have used fluences of 0.5, 1, and  $1.5 \times 10^{17}$  cm<sup>-2</sup>, providing Si concentration profiles with a peak at around 240 nm and initial silicon excess concentrations of about 5%, 10%, and 15%, respectively. Some few samples were implanted with lower fluences. The as-implanted samples were annealed at 1100, 1150, and 1200 °C under N<sub>2</sub> atmosphere in a conventional furnace for 1 h in order to nucleate and grow the Si precipitates. To study the time evolution of the process, a set of samples was annealed at 1150 °C for times ranging from 10 up to 240 min. PL measurements were performed at RT using the 488 nm (2.54 eV) line of an Ar-ion laser as the excitation source, with power density of 15 W/cm<sup>2</sup>. The emission was dispersed by a 0.5 m single spectrometer and detected by a cooled photomultiplier detector. All spectra presented here were obtained under the same conditions. Dark-field cross-sectional transmission electron microscopy (TEM) analyses were carried out with a 200 kV JEOL 2010 microscope in order to determine the NC size distribution in the annealed samples. The specimens were first mechanically thinned, and at a final stage they were ion-milled up to electron transparency through 5 keV Ar<sup>+</sup> bombardment.

## III. RESULTS

Light emission from the as-implanted samples was not detected, and TEM analyses showed no indications of crystallite formation. Samples annealed at temperatures below 1100 °C (not shown here) presented a PL signal several orders of magnitude lower than those coming from specimens treated at 1100 and 1150 °C. Our PL results show a strong RT emission at wavelengths ranging from 650 up to 1000 nm.

The PL spectra of five samples implanted to a fluence of  $1 \times 10^{17}$  cm<sup>-2</sup>, at different temperatures (RT, 400, 600, 700, and 800 °C), followed by an annealing at 1150 °C for 60 min, are shown in Fig. 1. We can observe that the samples implanted at RT and 400 °C present a very similar PL spectra, peaked at about 775 nm (1.6 eV). It is also clear from the figure that the PL peak of the samples implanted at temperatures higher than 400 °C is slightly redshifted. Moreover, the PL spectra width becomes broader towards the longer wavelength side, while the peak intensity decreases with increasing implantation temperature. The PL peak wavelength ( $\lambda_p$ ) as a function of the implantation temperature for all the annealing temperatures is represented in Fig. 2. In this plot, we can neatly distinguish two redshifts in the emission peak. One is related to the increasing annealing temperature, and

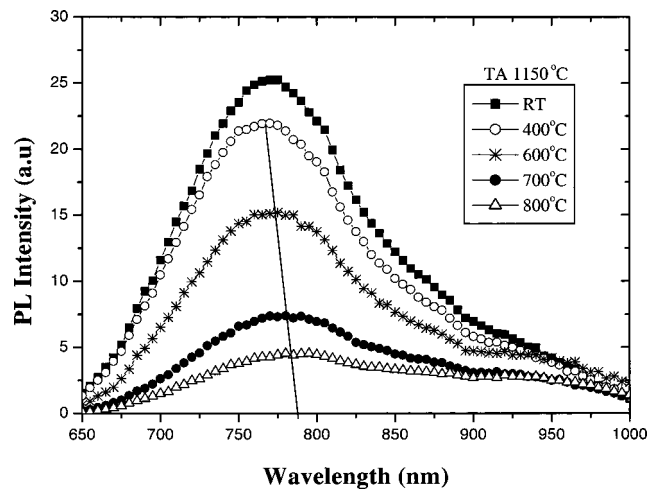


FIG. 1. RT PL spectra of SiO<sub>2</sub> samples implanted with 170 keV ( $1 \times 10^{17}$  Si/cm<sup>2</sup>) at RT, 400, 600, 700, and 800 °C, all thermal annealed at 1150 °C for 1 h under N<sub>2</sub> atmosphere in a conventional furnace. The straight line is a guide to the eyes, showing the redshift PL peak for hot implantations.

the other is related to the implantation temperature (from 400 to 800 °C). The inset shows the PL spectra for samples implanted at 600 °C and annealed at 1100, 1150, and 1200 °C, illustrating the wavelength peak redshift dependence on the annealing temperature.

The PL results for samples implanted to a fluence of  $1 \times 10^{17}$  cm<sup>-2</sup> are summarized in Fig. 3, where the PL intensity is plotted as a function of the implantation temperature for three different annealing temperatures (1100, 1150, and 1200 °C). We have found that after annealing at 1100 and 1150 °C, the integrated PL intensities present almost the same behavior. Both thermal treatments show a maximum PL intensity for implantation temperatures ranging from  $-200$  to 400 °C, and then exhibit a strong decrease for

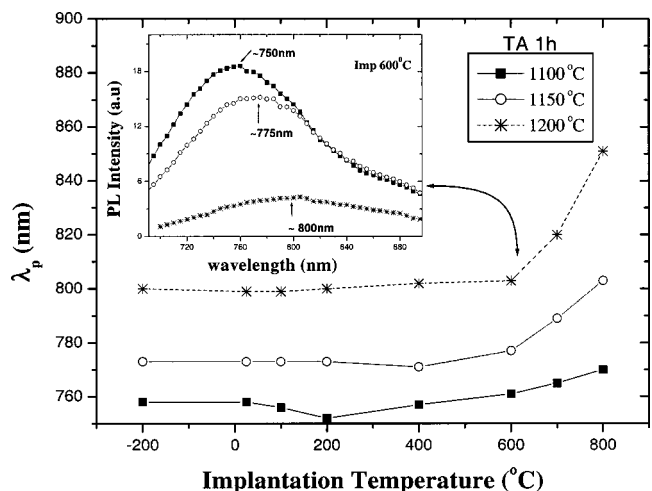


FIG. 2. PL peak wavelength ( $\lambda_p$ ) versus implantation temperature for samples implanted to a fluence of  $1 \times 10^{17}$  Si/cm<sup>2</sup> and thermal annealed for 1 h at temperatures of 1100 °C (full rectangle), 1150 °C (open circle), and 1200 °C (asterisk). The inset shows the PL spectra for three annealing temperatures of samples implanted at 600 °C. Lines are guides to the eyes.

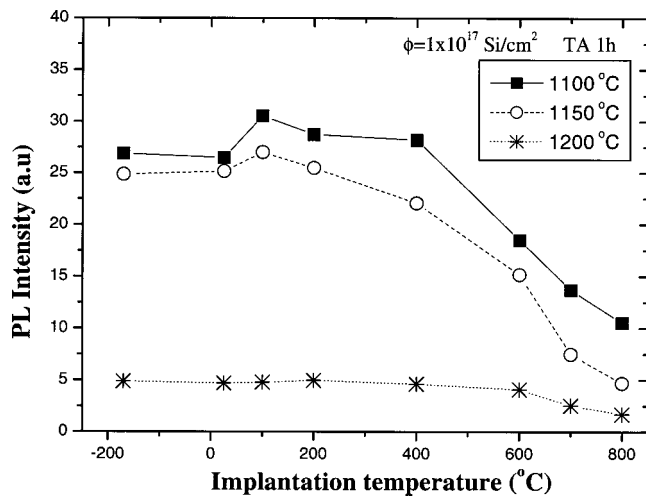


FIG. 3. PL intensity peak versus implantation temperature of samples implanted to a fluence of  $1 \times 10^{17} \text{ Si/cm}^2$  and annealed for 1 h at temperatures of 1100 °C (full rectangle), 1150 °C (open circle), and 1200 °C (asterisk). Lines are guides to the eyes.

higher values. For 1200 °C, the overall PL intensity drastically decreases, although the experimental curve still follows the same qualitative behavior of those corresponding to the other annealing temperatures.

In order to get more information about the implantation temperature influence on the Si NC PL, we have changed the initial silicon excess concentration in the  $\text{SiO}_2$  matrix, varying the implanted fluence from  $1 \times 10^{16}$  up to  $1.5 \times 10^{17} \text{ cm}^{-2}$ . In Fig. 4, the maximum intensity PL peak is plotted as a function of the implantation temperature for different fluences. The graphs (a), (b), and (c) in this figure display the results obtained for 1 h thermal treatments at 1100, 1150, and 1200 °C, respectively. Several statements can be established from this data: (i) For a given implantation temperature, the maximum PL intensity is always reached for 1100 °C thermal annealed samples. The exceptions

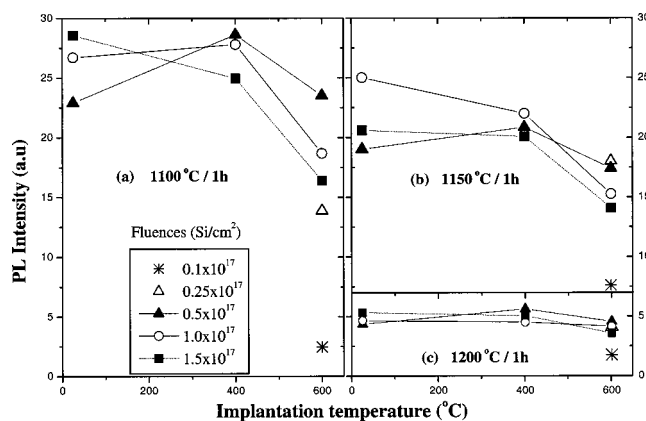


FIG. 4. PL intensity peak versus implantation temperature for different fluences:  $1.5 \times 10^{17}$  (full square),  $1 \times 10^{17}$  (open circle),  $0.5 \times 10^{17}$  (full triangle),  $0.25 \times 10^{17}$  (open triangle), and  $0.1 \times 10^{17} \text{ Si/cm}^2$  (asterisk). Samples were thermal annealed at (a) 1100, (b) 1150, and (c) 1200 °C. Lines are guides to the eyes.

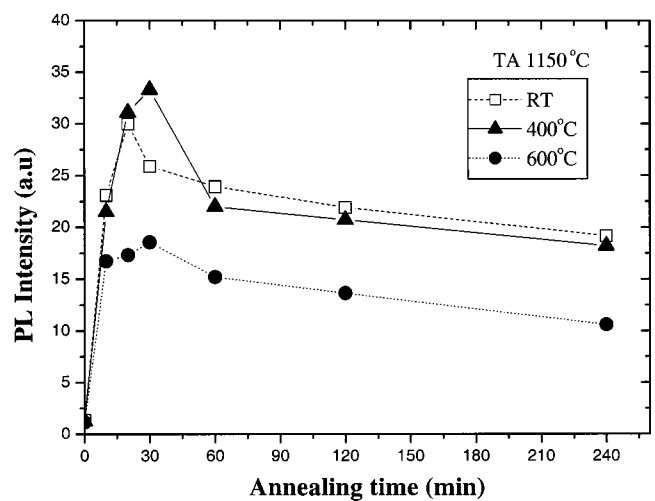


FIG. 5. PL intensity peak versus annealing time, from 10 to 240 min, for samples implanted with  $1 \times 10^{17} \text{ Si/cm}^2$  at RT (open square), 400 °C (full triangle), and 600 °C (full circle), and thermal annealed at 1150 °C. Lines are guides to the eyes.

are both lower fluences implanted at 600 °C ( $0.1$  and  $0.25 \times 10^{17} \text{ cm}^{-2}$ ), for which higher PL intensities are obtained for 1150 °C thermal treatment. (ii) Thermal annealing at 1200 °C [Fig. 4(c)] produces a very low PL signal, which is independent of the fluence and implantation temperature. (iii) For annealing at 1100 °C [Fig. 4(a)], the enhancement in the PL intensity can be obtained adjusting fluence and implantation temperature. That means we can achieve the maximum PL by implanting  $1.5 \times 10^{17} \text{ Si/cm}^2$  at RT or  $0.5 \times 10^{17} \text{ Si/cm}^2$  at 400 °C, (iv) It is important to note that there is an inversion in the PL intensity curves as a function of the fluence when we compare samples implanted at RT with hot implanted ones. There are no apparent relationships among the PL intensity, implantation fluence, and temperature. The tendencies change according to the implantation and annealing temperatures. This behavior can be observed in Fig. 4(a) as well as in Fig. 4(b).

The evolution of PL intensity as a function of the annealing time at 1150 °C is shown in Fig. 5. We present results corresponding to three different implantation temperatures: RT, 400, and 600 °C. This study has been made with samples implanted to a fluence of  $1 \times 10^{17} \text{ cm}^{-2}$ . After 10 min of thermal treatment, the PL signal is intense and shows almost the same value for the three annealing temperatures. By increasing the annealing time to 20 min, the PL intensity presents a new tendency: (i) at 600 °C, it almost does not change, but at RT and 400 °C it increases by 30% and 44%, respectively; and (ii) for 30 min of annealing time and implantation temperature at 400 °C, we observe the strongest PL signal. By further increasing the annealing time, all samples show a slow decrease in their PL intensities after 60 min of thermal treatment.

Structural information about Si NC size was obtained through the dark-field TEM analysis. The TEM micrographs have shown that larger mean size Si NCs have been formed when the samples were implanted at the same temperature, but annealed at higher temperatures. The same effect is

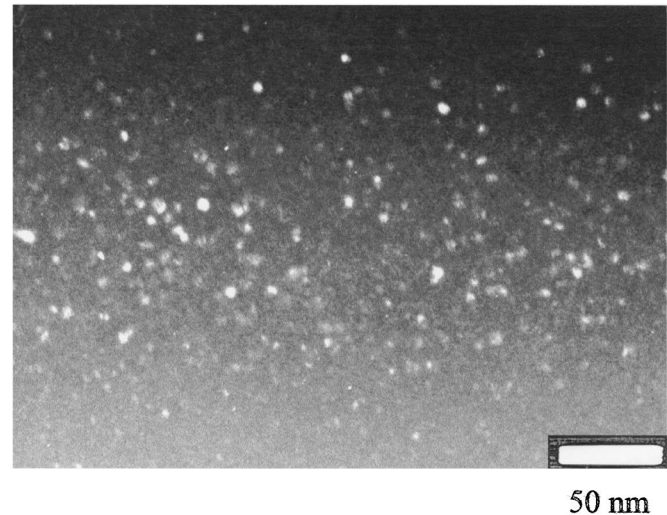
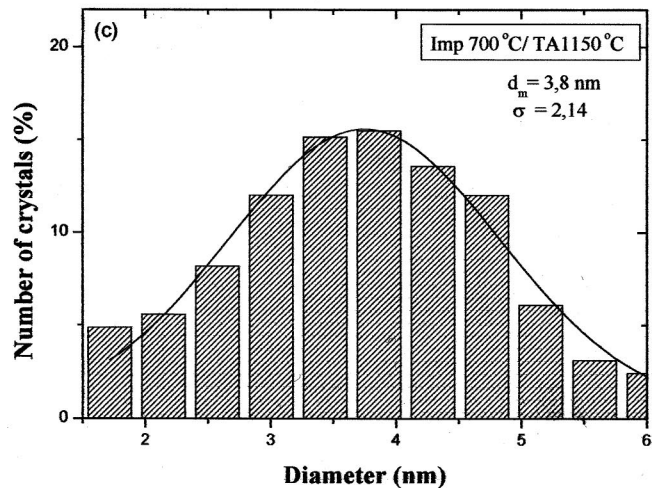
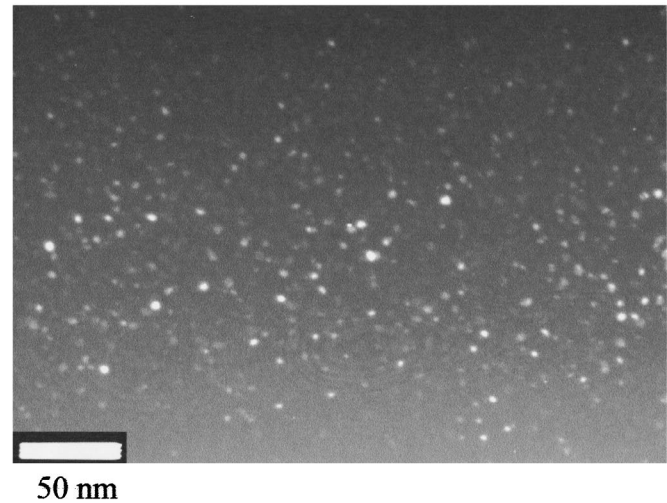
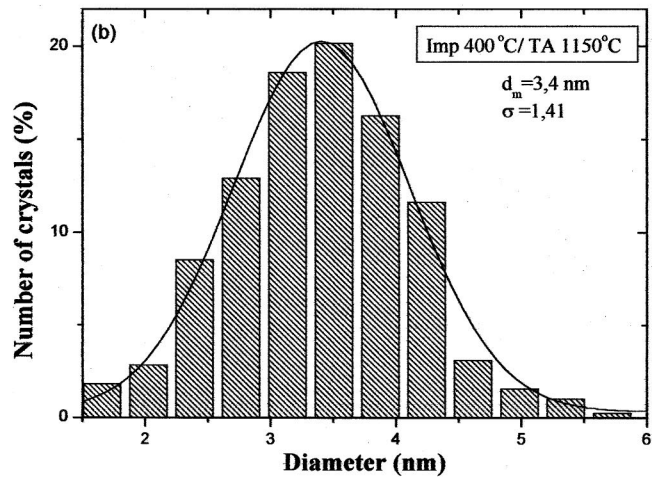
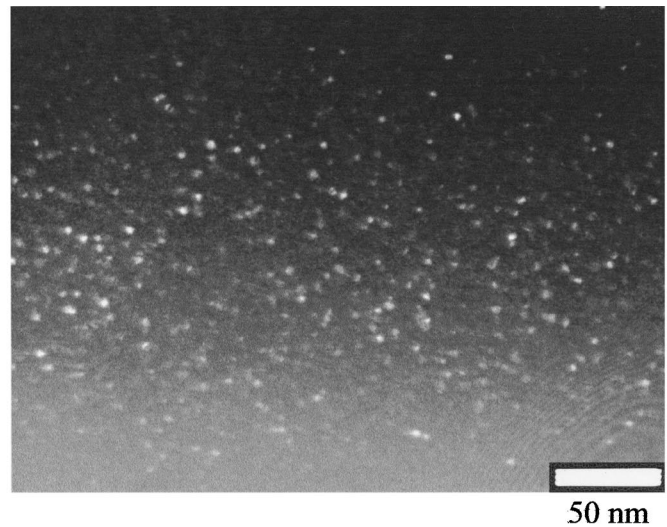
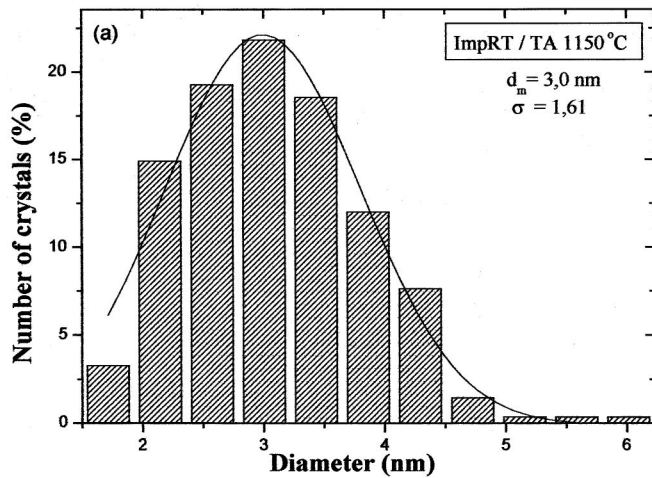


FIG. 6. Silicon size distributions obtained by dark-field TEM analysis from samples implanted at (a) RT, (b) 400 °C, and (c) 700 °C and thermal annealed at 1150 °C for 1 h. Corresponding TEM images are displayed at the right-hand side of each Si NC size histogram.

observed varying only the implantation temperature. The Si NC size distributions of three samples implanted at RT, 400, and 700 °C and annealed at 1150 °C are shown in Fig. 6 (the corresponding dark-field TEM images are shown). It is clear

from these results that the Si NC mean diameter increases with the implantation temperature. The same behavior was found when we compared samples implanted at 400 and at 700 °C, and annealed at 1100 °C.

## IV. DISCUSSION

### A. PL measurements

The very weak PL signals obtained from specimens annealed at temperatures below 1100 °C are probably due to the fact that in our system the Si phase begins to separate from SiO<sub>x</sub> around this annealing temperature.

It is important to recall that any PL comparison with other reports should be made only if the laser excitation energy is the same, because higher excitation energies would excite energy levels in particles of smaller size. Hence, the PL peak energy should appear at higher energies as compared to lower excitation energies.<sup>21</sup> In addition, different excitation intensities produce different PL intensities, a feature that is related to the saturation of some energy levels in the NCs.<sup>22,23</sup>

Our data show two different PL wavelength peak ( $\lambda_{\max}$ ) redshifts (see Fig. 2). One is related to the annealing temperature and the other is related to the implantation temperature. The PL redshift due to the annealing temperature had already been reported by other authors,<sup>4,24</sup> and is basically related to the size of Si NCs. The higher the annealing temperature, the larger the silicon grains. In agreement with the quantum confinement theory, the progressive redshift of the PL peaks with increasing crystal size is due to the reduction of the bandgap of the Si NCs approaching that of bulk crystalline silicon.

According to our results, the influence of the ion implantation temperature starts at about 400 °C, where the change in the  $\lambda_{\max}$  PL to higher wavelengths becomes evident. This fact can also be explained in terms of the Si NC growth, a feature that was confirmed by TEM analysis.

We have found (Fig. 3) that the PL intensity decreases with increasing annealing temperature (1100–1200 °C). In the same way, by fixing the annealing temperature, one observes that hot implanted samples at temperatures higher than 400 °C also present a decrease in the PL intensity with increasing implantation temperature. This can be explained on the following basis. It is known that different parameters determine the Si NC luminescence intensity, such as the number and size of the crystallites and/or competitive non-radiative processes. It has been reported that large NCs have smaller absorption cross section.<sup>8,25</sup> Although larger grains (~4.5 nm) have higher electronic density of states, the transition rate (oscillator strength) becomes smaller.<sup>8,25</sup> This is due to the fact that increasing the NC size, the absorption characteristics becomes similar to bulk Si, approximating the NC band structure to the Si indirect configuration. On the other hand, some authors have reported that  $P_b$  centers (Si dangling bonds located at the Si-NC/SiO<sub>2</sub> interfaces) or centers intimately related to them annihilate the radiative recombination in the Si NCs. The concentration of these centers and the PL intensity are inversely correlated.<sup>8</sup> It has been shown that in order to improve the Si-NC/SiO<sub>2</sub> interface, the defects related to such  $P_b$  centers must be annealed out.<sup>8</sup> Thus, even if the Si NCs have already reached an optimal size, an additional annealing time can be necessary. Increasing the PL emission intensity after annealing in forming gas ambient at temperatures 450–500 °C (not shown here) con-

firms this trend. For thermal treatments at 1200 °C, we verify that the PL intensity saturation is independent of the fluence and the implantation temperature, and the PL signal is weak when compared to that obtained from lower annealing temperatures. As was mentioned earlier, larger NCs have smaller cross sections for absorption; therefore, if the particles are larger, the less intense the luminescence will be. Of course, that is true after a certain critical size is achieved. For distributions with larger NCs, the energy may be transferred from small grains to larger ones more easily, depending on the distance between them.<sup>4,26</sup>

Next, we would like to discuss more specifically the results observed in the Fig. 4(a). It has been shown a clear inversion in the PL intensities as a function of implantation temperature for samples annealed at 1100 °C. In other words, the implantations at RT present higher PL signals as the fluence is increased, while hot implantations (400 °C or higher) present better results for decreasing fluences. An important result that we should point out here again is that  $0.5 \times 10^{17}$  Si/cm<sup>2</sup> implanted at 400 °C produces the same PL signal as  $1.5 \times 10^{17}$  Si/cm<sup>2</sup> at RT.

Iwayama *et al.* have reported that hot implanted samples contain more nucleation centers (silicon aggregates) formed during the implantation process than those implanted at RT.<sup>22</sup> When the implanted fluence and the annealing temperature are fixed, an increasing in the implantation temperature increases the number of Si NCs that will be grown in the SiO<sub>2</sub> matrix and, consequently, the interparticle spacing is reduced. It is known that the stability of small crystals depends on the balance between their volume and surface free energies and, consequently, their melting point may be much lower than the usual melting temperature.<sup>27–29</sup> Additionally, the reduced interparticle spacing can contribute to concentrate the silicon excess into larger crystallites after annealing at high temperature for ion implantation temperatures higher than RT. In this way, hot implantation facilitates the growth processes during annealing. The trend shown in Fig. 4(a) becomes clear if we admit that an optimal sized Si NC is achieved with lower silicon excesses due to the increase in the implantation temperature. The PL intensity peak obtained for  $0.5 \times 10^{17}$  Si/cm<sup>2</sup> is lower for implantations at 600 than 400 °C, probably because the optimal Si NC size was already achieved at 400 °C. For implantations at 600 °C [Fig. 4(a)], we can observe that at fluences increasing from  $0.5 \times 10^{17}$  up to  $1.5 \times 10^{17}$  Si/cm<sup>2</sup>, the PL decreases. Thus it was expected that lower fluences would give a better PL intensity after annealing at 1100 °C. For this reason, we have implanted  $0.25 \times 10^{17}$  and  $0.1 \times 10^{17}$  Si/cm<sup>2</sup> at 600 °C, but the measured luminescence intensity was lower. At these fluences, the grains formed after annealing are too small, presenting a higher surface/volume ratio. Consequently, the nonradiative defects on the Si-NC/SiO<sub>2</sub> interface can play a more intense role, decreasing the luminescence. This behavior has already discussed by Delerue *et al.*,<sup>30</sup> where they showed that the probability of nonradiative capture of a carrier by a single dangling bond is inversely proportional to the crystallite volume.

Another point to discuss is the PL intensity behavior by changing the annealing temperature [Figs. 4(a) and 4(b)]. We

observe that for annealing at 1150 °C, the PL intensity is lower than at 1100 °C because larger Si grains are formed. For most of the hot implanted fluences, the grain size became large enough so they can start to communicate with each other. The exceptions are the two lowest fluences, where for increasing NC size, we have found an increasing PL intensity.

On the other hand, implantations with fluences of  $0.25 \times 10^{17}$  and  $0.5 \times 10^{17} \text{ cm}^{-2}$  and annealed at 1150 °C [Fig. 4(b)] produce practically the same signal. For the higher fluence the effect of the surface/volume ratio is less pronounced; the grains have already exceeded their optimal size for emission.

For the time evolution of PL intensity (Fig. 5), the maximum PL has been obtained for about 30 min of annealing time. This is a sufficient time to grow the Si NCs to an appropriate size and to anneal out some of the interface defects. Longer annealing times yield crystallite sizes larger than the ideal. The slow decrease in the PL maximum after 1 h annealing may be related to the fact that the excess silicon amount in the SiO<sub>2</sub> matrix has already been consumed by forming the NC. Thus, the grains increase their sizes at lower rates.

## B. TEM analysis

The dark-field TEM micrographs shown in Fig. 6 help to clarify the discussion of Sec. A. TEM analyses have shown that samples implanted at the same temperature have large grains as the annealing temperature is increased (not shown), as expected. In addition, the higher the implantation temperature, (keeping the annealing temperature constant) the larger the Si NCs. As we mentioned in Sec. A, an increase in the implantation temperature produces a large number of nucleation centers in the SiO<sub>2</sub> matrix. However, if we observe the micrographs (see Fig. 6), we can verify that the number of NCs is reduced, and that the spacing between them is larger as the implantation temperature increases. This occurs because the initial nucleation centers are easily converted into larger ones, since they are closer each other and then coalesce.

In the PL measurements, the absorption cross sections for the different Si NCs depend on their size. The energy may be transferred from smaller to larger NCs which may reduce the PL intensity and produce some PL peak shift. The light energy source is fundamental to select the NCs that will emit. As we have stated above higher energies can excite small crystallites, which could be luminescent but not observable by TEM analysis. So, we would like to mention here the inconsistent method commonly accepted in the literature, which is to correlate directly the mean diameter of the NCs obtained from the silicon size distributions by TEM observations and the maximum PL peak energy obtained from PL measurements.

## V. CONCLUSIONS

We have investigated the influence of the implantation temperature on the photoluminescence of Si NCs embedded in SiO<sub>2</sub> matrix. This study was made systematically by

changing the implantation (temperature and fluence) and annealing (temperature and time) parameters. We have shown that the shape and intensity PL peak are dependent on the implantation temperature. A PL peak redshift was observed for higher implantation temperatures and was related to the Si NC growth. TEM analyses have demonstrated that the mean size of the Si NCs has a direct dependence on the annealing and implantation temperatures. Hot implantations facilitate the Si NC growth processes during the high annealing temperature. We have observed that there are no apparent relationships among the PL intensity, implantation fluence, and temperature. The maximum PL intensity was achieved by adjusting fluence and implantation temperature when the annealing temperature was of 1100 °C. Interestingly, we have achieved the same PL intensity with a three times lower fluence implanted at 400 °C than at RT.

## ACKNOWLEDGMENTS

The authors gratefully acknowledge financial support from FAPERGS (E. C. M., H. B.), FAPESP (E. R.), CNPq (H. B.), and CEFET-RS (U. S. S.). We are grateful to the GPO-IFGW-UNICAMP technical support, where the PL measurements were performed.

- <sup>1</sup>T. S. Iwayama, N. Kurumado, D. E. Hole, and P. D. Townsend, *J. Appl. Phys.* **83**, 6018 (1998).
- <sup>2</sup>T. Inokuma, Y. Wakayama, T. Muramoto, R. Aoki, Y. Kurata, and S. Hasegawa, *J. Appl. Phys.* **83**, 2228 (1998).
- <sup>3</sup>A. Kachurin, A. F. Leier, K. S. Zhuravlev, I. E. Tyschenko, A. K. Gutakovskii, V. A. Volodin, W. Skorupa, and R. A. Yankov, *Semiconductors* **32**, 1222 (1998).
- <sup>4</sup>F. Iacona, G. Franzò, and C. Spinella, *J. Appl. Phys.* **87**, 1295 (2000).
- <sup>5</sup>M. L. Brongersma, A. Polman, K. S. Min, E. Boer, T. Tambo, and H. A. Atwater, *Appl. Phys. Lett.* **72**, 2577 (1998).
- <sup>6</sup>T. S. Iwayama, T. Hama, D. E. Hole, and W. Boyd, *Solid-State Electron.* **45**, 1487 (2001).
- <sup>7</sup>T. S. Iwayama, K. Fujita, M. Akai, S. Nakao, and K. Saitoh, *J. Non-Cryst. Solids* **187**, 112 (1995).
- <sup>8</sup>B. Garrido Fernandez, M. López, C. García, A. Pérez-Rodríguez, J. R. Morante, C. Bonafos, M. Carrada, and A. Claverie, *J. Appl. Phys.* **91**, 798 (2002).
- <sup>9</sup>W. L. Wilson, P. L. Szajowski, and L. E. Brus, *Science* **262**, 1242 (1993).
- <sup>10</sup>R. E. Hummel and S.-S. Chang, *Appl. Phys. Lett.* **61**, 1965 (1992).
- <sup>11</sup>T. S. Iwayama, S. Nakao, and K. Saitoh, *Appl. Phys. Lett.* **65**, 1814 (1994).
- <sup>12</sup>H. Takagi, H. Ogawa, Y. Yamazaki, A. Ishizaki, and T. Nakagiri, *Appl. Phys. Lett.* **56**, 2379 (1990).
- <sup>13</sup>K. S. Min, K. V. Shcheglov, C. M. Yang, H. A. Atwater, M. L. Brongersma, and A. Polman, *Appl. Phys. Lett.* **69**, 2033 (1996).
- <sup>14</sup>J. G. Zhu, C. W. White, J. D. Budai, S. P. Withrow, and Y. Chen, *J. Appl. Phys.* **78**, 4386 (1995).
- <sup>15</sup>L. N. Dinh, L. L. Chase, M. Balooch, L. J. Terminello, and F. Wooten, *Appl. Phys. Lett.* **65**, 3111 (1994).
- <sup>16</sup>H. Morisaki, F. W. Ping, H. Ono, and K. Yazawa, *J. Appl. Phys.* **70**, 1869 (1991).
- <sup>17</sup>S. Hayashi, T. Nagareda, Y. Kanzawa, and K. Yamamoto, *Jpn. J. Appl. Phys., Part 1* **32**, 3840 (1993).
- <sup>18</sup>Y. Kanzawa, T. Kageyama, S. Takeoka, M. Fujii, S. Hayashi, and K. Yamamoto, *Solid State Commun.* **102**, 533 (1997).
- <sup>19</sup>Z. H. Lu, D. J. Lockwood, and J.-M. Baribeau, *Nature (London)* **378**, 258 (1995).
- <sup>20</sup>D. J. Lockwood, Z. H. Lu, and J.-M. Baribeau, *Phys. Rev. Lett.* **76**, 539 (1996).
- <sup>21</sup>S. Guha, S. B. Qadri, R. G. Musket, M. A. Wall, and T. S. Iwayama, *J. Appl. Phys.* **88**, 3954 (2000).

- <sup>22</sup>T. S. Iwayama, D. E. Hole, and I. W. Boyd, *J. Phys.: Condens. Matter* **11**, 6595 (1999).
- <sup>23</sup>D. Kovalev, J. Diener, H. Heckler, G. Poliski, N. Künzner, and F. Koch, *Phys. Rev. B* **61**, 4485 (2000).
- <sup>24</sup>T. Fischer, V. Petrova-Koch, K. Scheglov, M. S. Brandt, F. Koch, and V. Lehmann, *Thin Solid Films* **276**, 100 (1996).
- <sup>25</sup>C. Garcia, B. Garrido, P. Pellegrino, R. Ferre, J. A. Moreno, L. Pavesi, M. Cazzanelli, and J. R. Morante, *Physica E (Amsterdam)* **16**, 429 (2003).
- <sup>26</sup>S. Cheylan and R. G. Elliman, *Nucl. Instrum. Methods Phys. Res. B* **148**, 986 (1999).
- <sup>27</sup>A. N. Goldstein, *Appl. Phys. A: Mater. Sci. Process.* **62**, 33 (1996).
- <sup>28</sup>S. Veprek, *Thin Solid Films* **297**, 145 (1997).
- <sup>29</sup>D. Pacifici, E. C. Moreira, G. Franzò, V. Martorino, F. Priolo, and F. Iacona, *Phys. Rev. B* **65**, 144109 (2002).
- <sup>30</sup>C. Delerue, G. Allan, and M. Lannoo, *Phys. Rev. B* **48**, 11024 (1993).